Diameters and Velocities of Droplets Emitted from the Cu Cathode of a Vacuum Arc

Peter Siemroth, Michael Laux, Heinz Pursch, Jürgen Sachtleben, Martin Balden, Volker Rohde, Rudolf Neu

***Abstract*— Cathode spots of vacuum arcs emit material in the form of plasma as well as droplets. Generated by arcs burning at the first wall of fusion devices the droplets may effectively contaminate the fusion plasma. Essential characteristics of the droplets (diameter, velocity, and emission direction) and their interrelations are poorly known so far. In the present paper, a new approach of optical droplet investigation is presented. Emitted from a pulsed vacuum arc, the droplets fly vertically inside a drift tube against gravity, finally passing two consecutive light beams. The time-of-flight and the detected intensity of scattered light allow a simultaneous determination of droplet velocity and size. Different solid angle directions have been realized by turning the cathode with respect to the flight tube axis. Using this technique, the parameters of droplets emitted from a Cu cathode into different directions were obtained. Two distinct groups could be identified at smaller (<20°) and larger (>20°) angles between surface plane and emission direction, respectively. They exhibit different velocity distributions and different relations between the particle diameter and the emission velocity.**

Keywords—vacuum arc, light scattering, droplet velocities

I. Introduction

Arc discharges are an important erosion mechanism for the first wall of fusion devices [1]. Material is removed in the form of molten metal droplets and as a directed emission of plasma. While charged components have little chance of entering the magnetized plasma, the droplets can cross the magnetic field and contaminate central regions [2]. Estimates of the amount of the droplet material and its penetration depth are difficult to make, because the present knowledge of details of the droplet emission is insufficient.

The arc erosion on different metals has been studied experimentally as well as theoretically. Main properties of droplets were studied by several groups (e.g. [3], [4], [5], [6]). Models describing the emitted droplets were formulated based on the experimental results. Two types of processes are used to model the droplet production and acceleration: hydrodynamic ejection from the molten metal surface (e.g. [7], [8]) and acceleration of already emitted droplets by the interaction with a moving plasma (e.g. [9], [10], [20], [21]). Further results of droplet investigations on vacuum arcs might provide important improvements.

Manuscript received December 15, 2018.

Peter Siemroth, Michael Laux, Heinz Pursch and Jürgen Sachtleben are with the ArcPrecision GmbH, Schwartzkopffstrasse 2, 15745 Wildau, Germany. (email: info@arcprecision.com).

Martin Balden, Volker Rohde and Rudolf Neu are with the Max-Planck-Institut für Plasmaphysik, Boltzmannstrasse 2, 85748 Garching, Germany. Rudolf Neu is also with the Technische Universität München, Boltzmann-strasse 15, 85748 Garching, Germany.

The determination of droplet sizes is experimentally difficult because it must extend over many orders of magnitude with comparable accuracy. Often deposited droplets are investigated post mortem using optical or electron microscopy [11]. But molten droplets deform into complex shapes when they hit a collector surface. The volume of the impinging droplet can be derived by a detailed investigation of this deformation only [12]. There are indications that the distribution of the particle diameters could depend on the emission angle (e.g. [13]).

The published velocities range from below 30 m/s (e.g. [14], measured with moving collectors) up to nearly 1000 m/s (e.g. [15] measured with Laser Doppler Anemometry). Speed measurements with high-speed cameras for carbon particles yielded values between 10 and 370 m/s [16]. Our own observations [17] revealed intermediate speeds of 20 to 60 m/s depending on the material. Cameras have the problem that only hot and large particles are sufficiently bright to be detected. Additionally, the light of the spot itself outshines the radiation from the particle in the vicinity of the spot. There are hints that the velocity distribution depends on the emission angle as well [18].

Results of a simultaneous determination of the diameters and the velocities of individual particles as are required for the modelling of the passage of particles through the edge plasma of fusion devices are very rare (to our knowledge only in [13] and to a minor extend in [15]).

II. Experimental Setup

A. Experimental Apparatus and Arcing Conditions

The setup used here puts into effect a fairly new method to determine velocities and diameters of individual particles simultaneously. The schematic of the setup is shown in Fig. 1. The experiments apply a light scattering technique embedded in a time-of-flight arrangement to investigate the droplet emission from pulsed vacuum arcs. On their path (vertically up) the droplets are slowed down by the force of gravity. The (usually very narrow) solid angle range is selected by an aperture built into the drift tube, the velocity is derived from the time of flight between the cathode surface and the detector plane, and the size of the particle from the intensity of the scattered light. The vacuum apparatus is built from standard components and consists of three main sections. The lower part (a CF 4-way cross) contains the arc discharge assembly with a 50×60×10 mm³ Cu-cathode fixed on the flange in such a way that the active area of the cathode is located in the center of this 4-way cross. Thus, by turning the rotatable mounting flange, the angle under which the droplet emission is observed can be

selected freely in the range 0° to 90°. This angle is then fixed for the following experimental campaign. Therefore, velocities and diameters of particles can be obtained for distinct emission directions only. Electrically the chamber wall was connected as anode. A long drift tube was arranged as middle section oriented to the discharge. Droplets emitted in the right (i.e. pre-selected) direction can fly through the whole tube and reach the downstream detectors. Nevertheless, particles reflected at the wall during their path may also reach the observation volumes. Therefore, additional lamellas were used to narrow the lower part and catch reflected droplets. An aperture of 10×10 mm² was introduced close to the end of the drift tube to precisely define the solid angle range accepted (≈ 1.9° in linear extension). Due to the intended length of the drift tube, the ob-

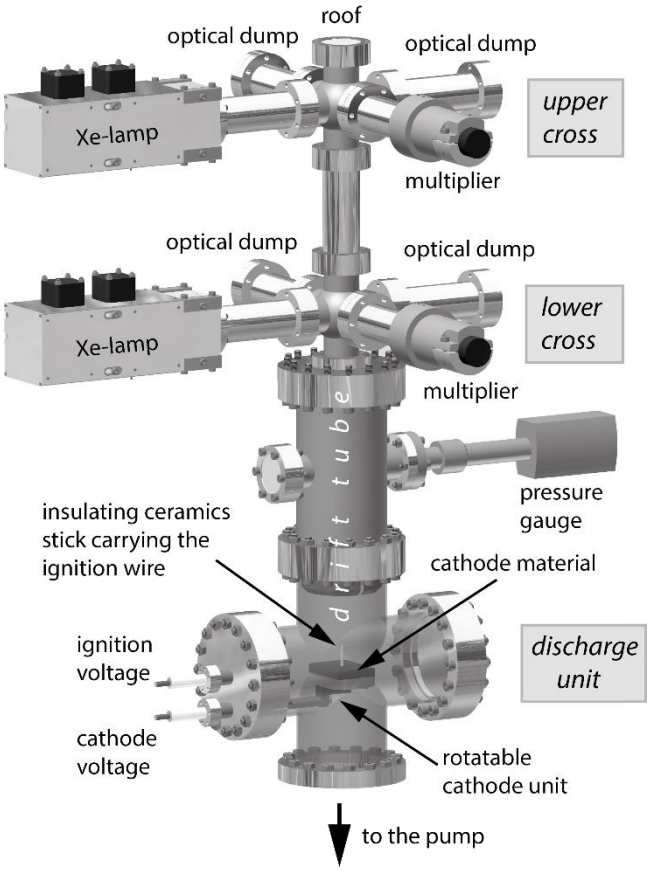

Fig. 1. Vacuum chamber, cathode unit, drift tube, and diagnostic crosses.

servations are carried out far from the discharge area and the droplets are probably cooled down enough to emit only a negligible thermal radiation. This was confirmed by observing the detector volume without illumination during several discharges. Even using a tenfold sensitivity only very few particles could be detected by their faint thermal emission resulting in a marginal systematic error for large particles.

The upper part of the vessel contains two identical optical particle diagnostics. Each of the small 6-way crosses is equipped with a light source for the uniform illumination of a defined measuring volume (approximately 20×20×11 mm³) and, perpendicularly, a suitable optical technique to detect scattered light from flying droplets. The distance between the cathode surface and the optical axis of the detection systems amounts 427 mm and 679 mm, respectively, constituting lower limits for the measured particle velocities (particles slower than ≈ 3 m/s topple over before reaching even the lower detector).

The applied arc current pulses are of rectangular shape (with slow variations of about ±10% of the roof value). The duration can be chosen to be 0.5 ms or e.g. 1 ms and the current maximum can be varied between 0.3 kA and 1 kA. During the discharge the burning voltage is typically several ten volts. The arc ignition electrode was fixed on the cathode mount. A high-voltage pulse of approximately 10 kV triggers a sliding discharge along an insulating ceramic rod to the cathode. At the larger currents the arcs obtained show multiple cathode spot features. Fig. 2 shows two examples of open-shutter photographs of the whole discharge at large current.

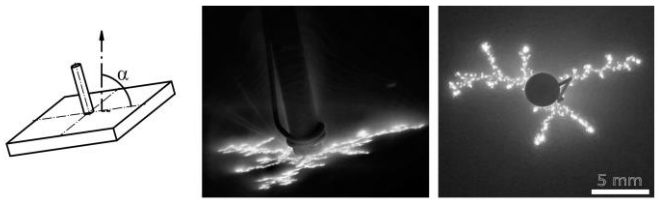

Fig. 2. Scheme of the inclined cathode arrangement showing the emission angle α (left), open-shutter photographs of the cathode during a discharge (current 0.5 kA, duration 1 ms) through a window (middle) and vertical open-shutter photograph of a discharge with 1 kA / 0.5 ms showing the radiation along the arc traces, taken earlier in another experimental device (rigth)

Typically, the base pressure inside the chamber is lower than 2×10^{-5} Pa. Discharge conditioning by numerous arcs prior to the measurement ensured that all contaminations (gases, oxides) are removed to have no influence on the arc mode (thereby ensuring the "clean-surface" type 2 tracks [11]).

B. Illumination and Detection Module for Particle Diagnostics

As known from former work, the diameters of macro particles cover a wide range between a few nanometers and several ten µm (see e.g. [2, 11, 21]). To be able to detect small droplets, the intensity of the light source must be as high as possible. White-light has the advantage that complex structures of Mie-scattered light for different wavelength, polarization, and angle are smoothened away. For this purpose, a Xenon short arc lamp model XBO® R 300 W by Osram was used. After extensive optimizations it was possible to achieve a homogeneous luminance distribution using a single lens and a collimation of the primary beam. Within the parallel beam 38% of the total light emitted by the lamp enter the observation area. Strong efforts were made to suppress most of the stray light by plating the collimating optics and the active areas of the light dumps with a coating of Vantablack® by Surrey NanoSystems.

To detect the two scattering signals, two photomultipliers (Hamamatsu Photonics, H10492-003) were used. The spectral sensitivity ranges from 300 nm to 700 nm and covers the emission range of the white-light source. The detection system must register the scattered light as completely as possible but, at the same time, avoid all stray light sources, particularly the

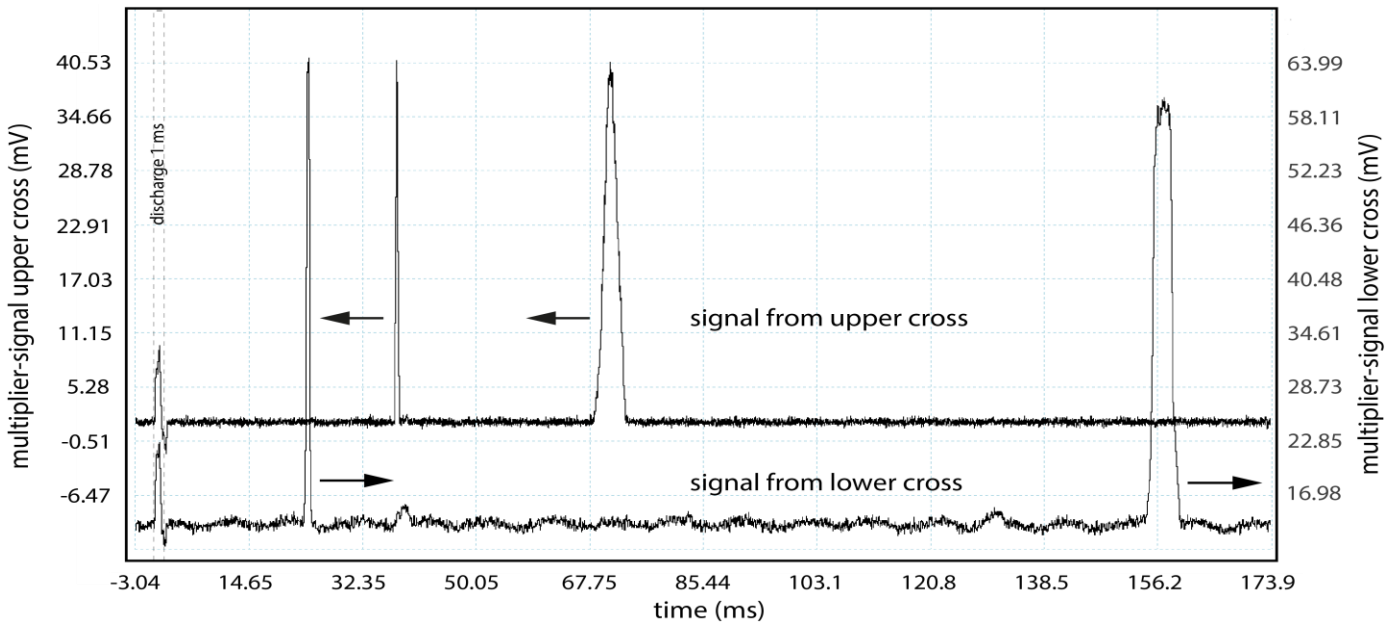

Fig. 3. Cutout of an original oscillogram of the multiplier signals of the upper (black, left scale) as well as the lower (dark gray, right scale) cross for the 188 ms following the discharge (processed by low-pass filters). Arc current 0.5 kA. Two passages of a particle are seen in each signal channel.

light reflected from corners of the dumps. The central area of the observation volume is mapped to the multiplier entrance window by a large aperture aspherical lens. By mounting the lens immediately behind the collimator inside the vacuum, it could be achieved that the central area of the measuring volume is imaged to the outer surface of the vacuum window. A slit diaphragm tailored manually ($\approx 1\text{mm} \times 10\text{mm}$) excludes straylight and defines the region of observation covered by the multiplier.

III. Measurement and Data Processing

The successive emission of particles of different size and velocity from the cathodic spot was observed by the registration of time series of the two multiplier output signals starting at about 50 ms before the breakdown and lasting typically until 450 ms after the ignition of the arc. A 4-channel USB-oscilloscope from PicoScope® (model 5442B) was used to monitor the multiplier signals representing the intensities of scattered light. The sampling interval was 96 ns (rate 10.42 MSample/s) at a resolution of 14 bits. A voltage range of ±500 mV was used for the channels measuring the multiplier signals.

Fig. 3 demonstrates the cutout of the oscillogram of an arc of 0.5 kA for a relevant time interval (here beginning just before the discharge and reaching until about 190 ms after the discharge). Two pairs of subsequent peaks are prominent. The first one produced presumably by a particle moving up, the second from a particle falling back down. Peak intensities are roughly comparable. The raw signals (w/o the filtering applied for Fig. 3) exhibit a noticeable noise of about ±3 mV, a slowly varying background of about 10 mV, and oscillatory contributions from the modulated primary light (recognized by the frequencies: 50 Hz, 100 Hz, and 150 Hz). The data have been reworked in four steps:

1) Data are restricted to times after the end of the discharge until 450 ms.
2) Each time-series is divided into consecutive intervals of 30 µs, the voltages in each of these intervals are sorted, and a fraction of the highest and a fraction of the lowest values are discarded (1/4 each). The remaining voltages are averaged to build the new data pair together with the mid-time of the interval.
3) A polynomial of order 4 is fitted to this new data set and subtracted to compensate for the background.
4) Amplitudes and phases of a 50 Hz, a 100 Hz, and a 150 Hz oscillation are fitted and subtracted.

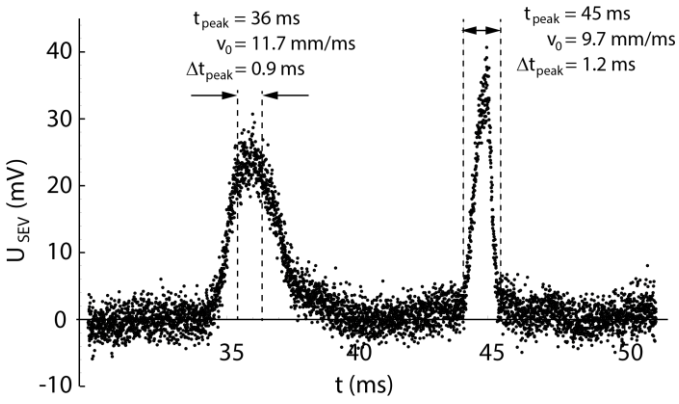

Fig. 4. Intensity of scattered light vs. time for signals from the lower cross after processing. Two example peaks: the right peak fits the ballistics exhibiting the correct duration for its time of occurrence; the left one is much too long for its arrival time.

The resulting set of corrected data shows clear peaks at certain times t_{peak} with respect to the beginning of the discharge (t=0). They indicate particles passing an observation window at height

h (here 427 mm). As a first approximation it is assumed that the duration of the discharge (typically 1 ms) is short as compared to t_{peak} and all particles are treated as emitted at t=0 (instead of their real emission anytime during the discharge). The peaks have a temporal width Δt_{peak} corresponding to the time it takes the particle to pass the observed width of the window (here ≈ 11 mm). A simple ballistics that takes only the gravitational force into account, determines a relation between Δt_{peak} and t_{peak} assuming that the particle can be treated as a point mass starting at the cathode with the vertical velocity v_0. This velocity is then

$$v_0(t_{peak}) = {}^{g}/_{2}\, t_{peak} + {}^{h}/_{t_{peak}} \qquad (1)$$

and the velocity v_{peak} in the window becomes

$$v_{peak} = v_0 - g \cdot t_{peak} \qquad (2)$$

with g the gravitational acceleration and h the height of the window above the cathode plane. A good approximation for the time it takes the particle to pass a window having the width Δh is then

$$\Delta t_{peak} \approx \Delta h / v_{peak} \qquad (3)$$

assuming that $\Delta h << h$. It has to be admitted that the determination of the width Δh of the observation window introduces the largest (systematic) uncertainties.

Unfortunately, not all peaks fulfil the requested relation between t_{peak} and Δt_{peak} as the examples in Fig. 4 demonstrate. Too wide peaks are produced by particles that stay too long in the observation volume as is expected from their arrival time. This may be caused by collisions of the particles with the vessel walls or other inner structures on their way from the cathode to the detector plane. Therefore, those particles must be excluded from the further data evaluation.

A. The determination of the particle diameter from the output signal of the multiplier

The intensity peaks produced by passing particles exhibit quite a variety of shapes and are embedded in the remaining noise. The identification of relevant peak windows proved to be done best by using an interactive Python program. All the other steps have been automated using MATHEMATICA®. To finally evaluate the parameters of the individual peaks a Gaussian was fitted to the data of each peak window providing the temporal position, the height, and the width of the peak. In the fortunate case of the appearance of the same particle in the lower and the upper detectors (see e.g. Fig. 3; all four peaks may belong to the same upwards flying and downwards falling particle), both the emission velocity and the real emission time of the investigated particle can be deduced.

Furthermore, from the height of the peak – representing the intensity of the light scattered by this particle – the particle diameter can be inferred. For the evaluation of the intensity $I(d,\lambda)$ of scattered light the theory of Mie scattering must be applied because the range of diameters of the scattering droplets exceeds the range of wavelengths of the primary light as well as the range of wavelengths detected by the multiplier (possible ratios d/λ of particle diameters and wavelengths vary at least from 0.01 to 100). The intensity of light scattered by a spherical particle of (complex) refractive index m into a direction in space given by (φ, θ) can be numerically calculated as a function of the parameter $x = k \cdot r = 2\pi/\lambda \cdot d/2$ (the product of wavenumber and particle radius) using the formalism described in [19]. θ is the scattering angle between incoming light and the direction to the detector and φ the polar angle of the detector's direction. In our cylindrically symmetric arrangement (around an axis going through the particle and oriented parallel to the beam of incoming light) the result does not depend on φ, therefore, it can be set to zero for simplicity. The scattering angle θ is very close to π/2. The angular apertures of the beams of illuminating light on the one hand and of scattered light on the other hand require the averaging of the intensities over these angular apertures (typically ±2.5°). The current lateral position of the vertical pathway of a light scattering particle in the observation volume also affects the scattering angle. Unfortunately, this position cannot be measured and, therefore, has to be accounted for as a systematic error.

The broadband source of white light (λ = 0.3…0.8 µm) and the finite acceptance range of the multiplier (λ = 0.3…0.6 µm) require an integration of the scattered light extending over the convolution of these two regions of wavelengths taking the emissivity of the lamp and the sensitivity of the multiplier into account. Fortunately, this averaging flattens the prominent structures in the Mie-region ($k \cdot r = \pi d/\lambda \approx 1$). Having all this at hand the dependence of the multiplier signal measuring the scattered light on the diameter of the scattering particle can be calculated for Cu (adopted m = 1.2-2.2i) as an example (Fig. 5).

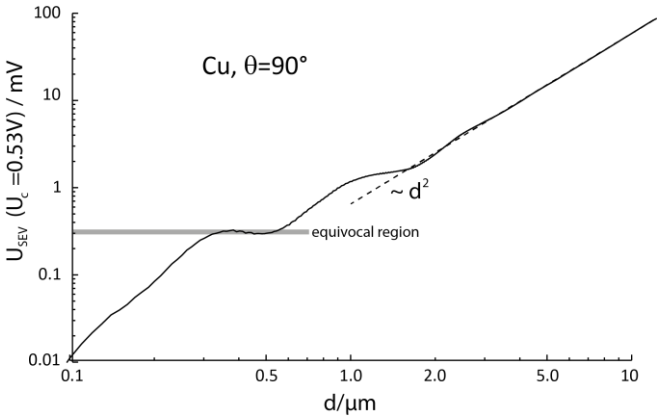

Fig. 5. Calculated multiplier output U_{SEV} (as measure for the intensity of scattered light) vs. particle diameter

For large diameters the curve approaches asymptotically a parabola $U_{SEV} \sim d^2$ as expected. Around $U_{SEV} \approx 0.3$ mV a small equivocal region exists rendering the inversion of signal-voltages into diameters impossible.

An estimate of the intensity of light scattered by a Cu-sphere combining the emissivity of the lamp, the properties of the optical systems, and the sensitivity of the multiplier yields a multiplier signal of about 1mV for a particle of 1µm diameter in good agreement with the results of the Mie-scattering simulation.

The curve in Fig. 5 has to be used to determine the particle diameter from an observed multiplier voltage (with the exception of the small equivocal region). For the example mentioned earlier (Fig. 3) the intensity of scattered light measured by the multiplier output-signal (53 mV for the lower cross, 41 mV for the upper) results in a diameter of between 8 and 9 µm.

B. Particles falling through the detectors

Particles falling through the drift tube have also been observed (compare in Fig. 3 the second peaks for both measured positions) passing the upper detector prior to the lower one. Of course, this could reflect the down-hill part of the particle's ballistic path after passing the apex. But there is not much height left between the upper detector-cross and the top roof of the vessel. Therefore, several particles will unavoidably impinge at the roof surface having a vertical velocity that can be calculated. Their sticking cannot be ascertained, consequently, some of them might also be reflected in-elastically suffering a loss of energy and momentum. If the two peaks belong to the same falling particle on its way down or not can be investigated applying the same ballistic techniques as for the direct shot. The resulting emission velocity at the roof can be compared to the impact velocity to estimate the loss parameters. In the example shown in Fig. 3 the particle hits the roof at 41 ms with a velocity of 17.8 m/s. After reflection it moves down with only -1.8 m/s. This implies a loss of 90% of the momentum, assuming that the integrity of the particle during the wall impact is ensured. It is worth noting that particles sticking to the roof can be detached from the surface at almost any time (e.g. by mechanical vibrations or by a running discharge) to fall down with an "emission" velocity close to zero.

IV. Results and Discussion

The distribution of the number of particles having an observed diameter (deduced from the multiplier output voltage U) follows a potential law with an exponent of -3.74 ± 0.11 (Fig. 6). The comparison of this exponent with a typical value of -3.4 reported in the literature [11] is satisfactory and suggests that the simple relation $U \sim d^2$ between the measured intensities (multiplier voltages) and the diameters of the scattering particles holds as a good approximation: the intensities are roughly proportional to the projected particle areas.

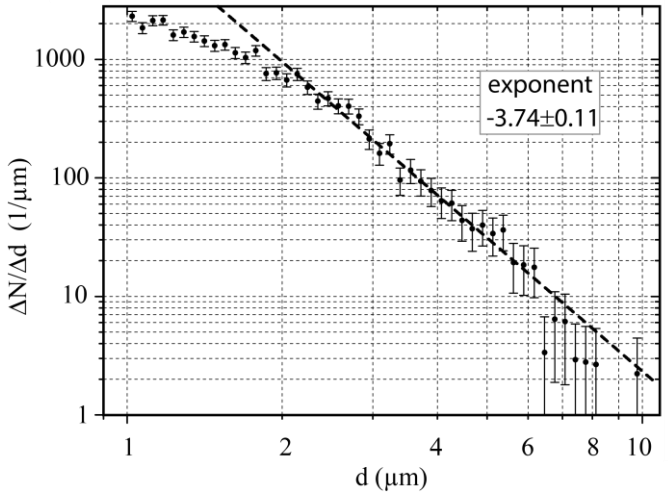

Fig. 6. Log-log distribution of the diameters of 2064 accepted individual particles showing a potential law for 1.5 µm ≤ d ≤ 10 µm.

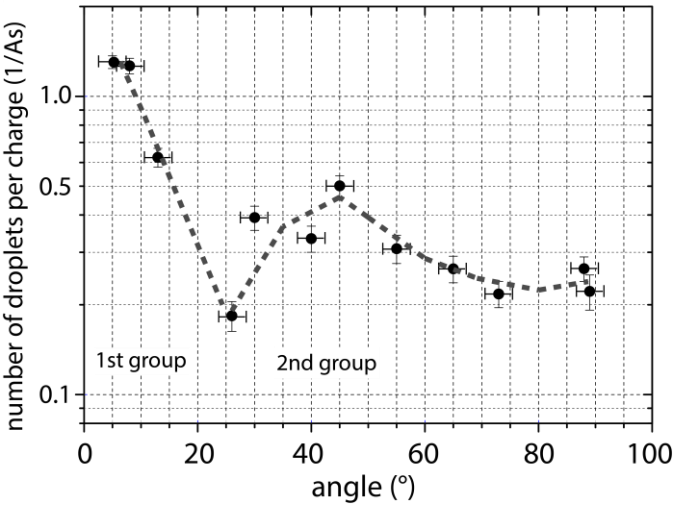

Fig. 7. Angular distribution of emitted particles composed of two groups at shallow (<20°) and steep (>20°) angles, respectively.

Campaigns of about 100 discharges each have been carried out for several pre-selected angles to investigate the dependence of particle emission on the angle between the emission direction and the cathode plane (compare Fig. 2 left; small values represent shallow emission!). In principle the number of particles emitted per discharge flying into a given direction declines with the angle (Fig. 7). But, despite the quite small number of angular positions, the apparent minimum around 20° suggests that two distinct groups of particles are suspected to contribute to the result (indicated by the dashed curve to guide the eye in Fig.7; consider the error bars). The first group includes particles emitted shallower than 20° (comparable to the distribution reported in [13]), the second group contains those flying steeper than 20° (also found in [14], but not in [5]). Although the second distribution declines at larger angles, an appreciable number of particles is still emitted at very steep angles (with respect to the surface).

The distributions of the measured emission velocities $v_{z,0}$ shown in Fig. 8 for the shallow and steep angles, respectively, differ from each other. More specifically, a re-directing acceleration process seems to change the magnitudes of the velocities as well as their directions. In a multiple-spot arc the interaction of the slowly (10…100 m/s) flying particles with fast (≈ 10^4 m/s) plasma jets passing them represents such a process: particles may surf the plasma clouds (see e.g. [9], [10]).

Fig. 9 shows all individual particle diameters inferred from the amount of scattered light versus the emission velocity derived from the flight duration for a large number of particles having shallow or steep angles, respectively. For a given diameter an upper limit $v_{0,max}$ of the emission velocity seems to exist. This limit is lower for larger diameters. Shallow particles seem to concentrate close to this border, whereas particles

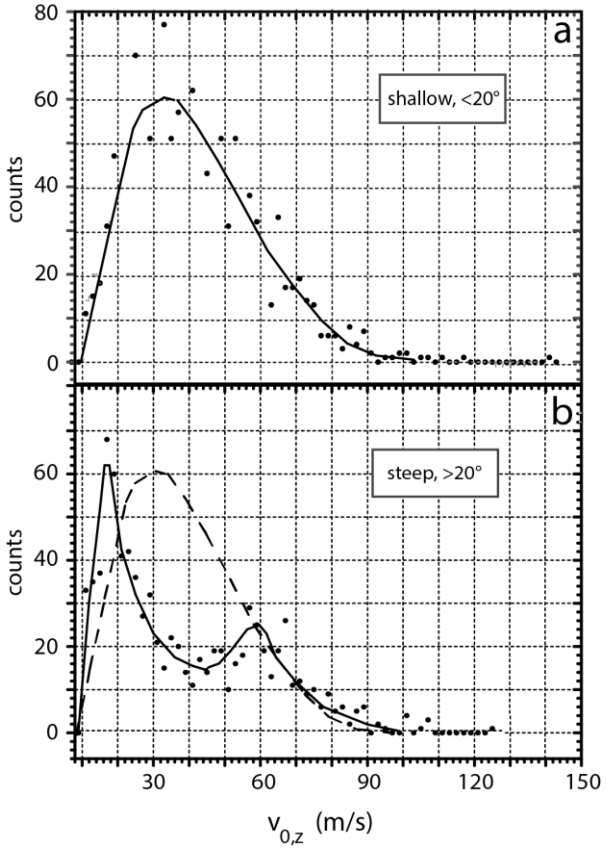

Fig. 8. Distributions of velocities $v_{z,0}$ for shallow and steep angles with respect to the cathode surface. (a) Angles <20°. (b) Angles >20°. Solid lines are for guiding the eye, and the dashed line in (b) is copied from (a) for comparison.

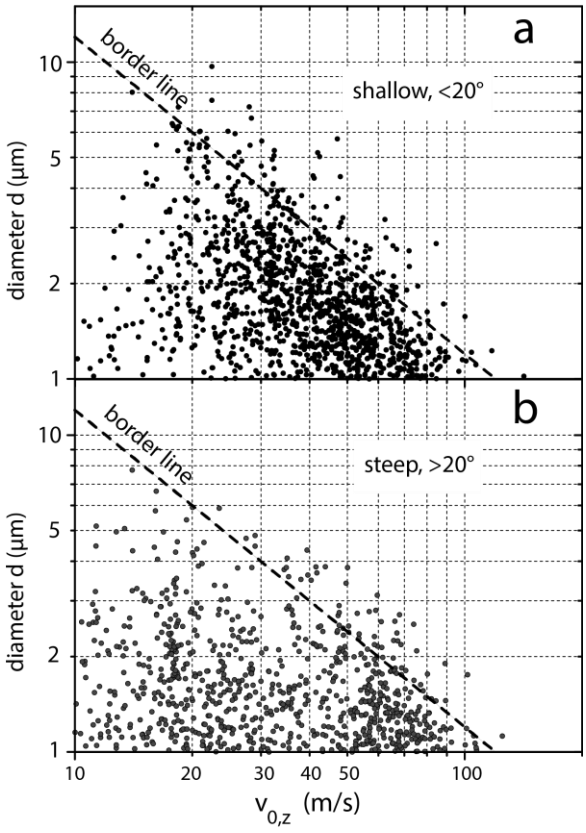

Fig. 9. Measured particle diameter vs. emission velocity for shallow and steep angles in relation to the cathode surface. (a) Angles <20°. (b) Angles >20°.

flying at steeper angles avoid the border and fill the parameter space at lower diameters and lower velocities.

The emerging borderline falls with $v_{0,max}$ in such a way that the velocity $v_{0,max}$ is proportional to the inverse of the particle diameter.

This relation cannot be understood by the idea of a hydrodynamic acceleration of droplets at the crater rim alone (e.g. [7], [8]). Additionally, the acceleration resulting from the interaction of the fast streaming plasma originating from the spots on the cathode must be taken into account. This drag-force accelerates the emitted particles vertically. A rough estimate of the force yields

$$F_z = m\,\Delta v_z/\Delta t = m\,(v_{z,0} - 0)\,/\tau \sim d^3\,v_{z,0} \qquad (4)$$

with m the mass of the particle and τ the duration of the acceleration process. Here is assumed that the vertical velocity of the particle is 0 prior to the thrust. If the force is applied by the pressure of a plasma stream it supposed to be (among others) proportional to the exposed area of the particle

$$F_z \sim d^2 \qquad (5).$$

A comparison with (4) implies $v_{z,0} \sim 1/d$ as seen for the limiting line in Fig. 9.

Deviations from the exponent -1 can be caused by the more complex dependence of the intensity of scattered light on the size of the particle (here assumed as $I \sim d^2$) as described by Mie's theory. Additionally, the mere appearance of the fastest particle's points to the action of an acceleration mechanism.

V. Conclusion

An experimental setup able to measure in-situ diameters and velocities of individual droplets emitted from vacuum arcs was developed and successfully tested. It is based on a drift tube arrangement combined with a time-of-flight technique and the registration of light scattered by the droplets. White light sources were used to smooth the complex dependence of scattered light on the size of particles as described by Mie's theory. From the presented results the following conclusions can be drawn:

1) The installed technique was able to register cathode droplets with diameters larger than 0.5 µm in flight. The measured velocities reached from 10 to 120 m/s.
2) The distribution of the number of particles with the particle size (represented by the observed peak-intensities) follows a potential law with an exponent of about -3.74±0.11. This exponent is comparable to values in reference [2] and supports that the simple relation $U \sim d^2$ between the

measured intensities and the diameters of the scattering particles is a good approximation.

3) The angular distribution of emitted particles declines with the angle against the cathode surface and may consist of a small-angle group (≤20°) and a group for large angles (>20°). An appreciable quantity of particles is emitted even at steep angles.
4) For a given diameter an upper limit $v_{0,max} = \max(v_{z,0})$ of the emission velocity seems to exist, that is lower for larger diameters. An emerging borderline is approximately proportional to the inverse particle diameter.
5) The conclusion 4) has implications for the behaviour of arc produced particles passing the edge plasma of fusion devices. One outcome of the simulations of those particles is, that the critical perpendicular velocity for just reaching the central plasma scales like the inverse particle radius [2]. Therefore, the existence of a velocity limitation and the finding that this limit is lower for larger particles can prevent the deep penetration of arc-produced particles into a fusion plasma.

ACKNOWLEDGMENT

The work is carried out within the framework of a contract between the Arc Precision GmbH and the Max-Planck-Institut für Plasmaphysik, Garching. The authors would like to thank the "Department Photonics, Laser and Plasma Technology" of the Technical University of Applied Sciences, Wildau, for the temporary deployment of the pulse power source for operating the vacuum arcs. We thank Oliver Laux for providing the Python evaluation routine. Special thanks to Karin Siemroth for her support of design and construction of the experimental setup.

REFERENCES

[1] V. Rohde, M. Balden, the ASDEX Upgrade Team, "Arc erosion of full metal plasma facing components at the inner baffle region of ASDEX Upgrade", *Nuclear Materials and Energy*, vol. 9, pp. 36-39, 2016.

[2] M. Laux, M. Balden, and P. Siemroth, "Modification of arc emitted W-particles in the scrape-off layer plasma", *Phys. Scr.*, Volume 2014, Number T159, 2014. DOI:10.1088/0031-8949/2014/T159/014026.

[3] J.E. Daalder, "Components of cathode erosion in vacuum arcs"; *J. Phys. D: Appl. Phys.*, vol. 9, pp. 2379-2395, 1976.

[4] T. Utsumi, J. H. English, "Study of electrode products emitted by vacuum arcs in form of molten metal particles", *J. Appl. Phys.*, vol. 46, no. 1, pp.126-131, 1975. DOI: 10.1063/1.321333.

[5] D.T. Tuma, C.L. Chen, D.K. Davies, "Erosion products from the cathode spot region of a copper vacuum arc", *J. Appl. Phys.*, vol. 49, no.7, pp. 3821-3831, 1978.

[6] J. Kutzner, H.C. Miller, "Cathode erosion and mass balance in a vacuum arc", *Proc. XVth ISDEIV*, Darmstadt, Germany, 1992, pp. 321-325.

[7] E. Hantzsche, "Droplet emission from vacuum arc spots", *Proc. VIIth ISDEIV*, Novosibirsk, Soviet Union, 1976, pp.324-327.

[8] H T C Kaufmann, M D Cunha, M S Benilov, W Hartmann and N Wenzel, "Detailed numerical simulation of cathode spots in vacuum arcs: Interplay of different mechanisms and ejection of droplets", *J. Appl. Phys.*, vol. 122, no. 16, pp. 163303, 2017.

[9] R. L. Boxman, S. Goldsmith, "The interaction between plasma and macroparticles in a multicathodespot vacuum arc*", J. Appl. Phys.*, vol. 52, no.1, pp. 151-162, 1981. DOI: 10.1063/1.328467.

[10] M. Lukovnikova and P. Siemroth, "Interaction of microdroplets with a plasma of vacuum arc discharge", *Proc. XXIXth Conference on Plasma Physics and CF*, Zvenigorod, Russia, 2002, unpublished.

[11] A. Anders, "Cathodic Arcs: From Fractal Spots to Energetic Condensation", Springer Series on Atomic, Optical, and Plasma Physics, Book 50, New York, 2008, [Online] Available: https://www.springer.com, e-ISBN: 978-0-79108-1.

[12] J.E. Daalder, "Cathode erosion of metal vapor arcs in vacuum", Thesis TU Eindhoven, 1978.

[13] J. E. Daalder, J. C. A. M. Gordens, "Velocities of macroparticles generated in the cathode spot region of a vacuum arc", Proc. XVIth ICPIG, Düsseldorf, pp. 274-275, 1983.

[14] I.I. Aksenov, A.A. Andreev, V.A. Belous, V.E. Strelnickij, and V.M. Khoroshikh, "Vacuum arc: sources of plasma, coating deposition, surface modification", Publisher: Naukowa Dumka, Kiev, Ukraine, 2012. ISBN 978-966-00-1134-2.

[15] S. Shalev, S. Goldsmith, and R.L Boxman, "In situ determination of macroparticle velocities in a copper vacuum arc*", IEEE Trans. Plasma Sci.*, vol. PS-11, no. 3, pp. 146-151, 1983.

[16] T. Schülke and A. Anders, "Velocity distribution of carbon macroparocles generated by pulsed vacuum arcs*", Plasma Sources Sci. Technol.*, vol. 8, pp. 567-571, 1999.

[17] M. Marx, "Investigation of bipolar vacuum arcs on first-wall-materials" (Untersuchung von bipolaren Vakuumbögen auf Erste-Wand-Materialien), Diploma thesis, Technical University of Applied Sciences Wildau, Germany, April 2011.
[Online] Available https://d-nb.info/1114277754/34.

[18] B. Gellert, E. Schade, "Optical investigation of droplet emission in vacuum interrupters to improve contact materials", *Procc. XIVth ISDEIV*, Santa Fe, USA, 1990, pp. 450-454.

[19] H. C. van de Hulst, "Light Scattering by Small Particles", Dover Publications, Inc., New York, USA, 1981.

[20] A. Anders, "Growth and decay of macroparticles: A feasible approach to clean vacuum arc plasmas*?", J. Appl. Phys.* Vol. 82, pp. 3679-3688, 1997. DOI: 10.1063/1.365731.

[21] S. Anders, A. Anders, K. M. Yu, X. Y. Yao, I. G. Brown, „On the macroparticle flux from vacuum arc cathode spots", *IEEE Trans. Plasma Sci.*, vol.21, no.5, pp .440-446, 1993.

Peter Siemroth was born in Berlin Germany on May 11, 1948. He received the Dipl. Phys. degree 1973 from the Moscow Lomonossov University and the doctorate degree from the Academy of Sciences of the GDR. From 1973 until 1989, he was with the Central Institute of Electron Physics in Berlin. In 1990, he joined the Fraunhofer Institute for Materials Physics and Surface Eng. (IWS) in Dresden. In 2003, he was one of the founders and since then director of the enterprise "Arc Precision GmbH", recently located in Wildau near Berlin. His main research interests are in the investigation of vacuum arc processes and in various applications of arc discharges.

Michael Laux was born in 1948 in Schwerin, Germany. He received his first degree and his PhD in theoretical solid state physics from the Technical University, Dresden. Since 1974, he was with the plasma and surface science department of the Central Institute of Electron Physics. He spent work stays at the Kurchatov Institute, Moscow, the JET project, Abingdon, and the Forschungszentrum Jülich working on plasma surface interaction in fusion devices. Since 1992, he worked for the Max-Planck-Institute of Plasma Physics, Garching, on the field of divertor physics and from 2003 until his retirement for the W7-X project, Greifswald.

Heinz Pursch was born in 1953. He received the M.S. degree from Humboldt-University, Berlin, Germany, in 1976 and the PhD from the Academy of Sciences, Berlin, in 1985. From 1976 to 1991, he was with the former Central Institute of Electron Physics, Berlin, where he was involved in vacuum arc research and current interruption phenomena. During 1992, he was with the Institute of Welding Technology of the Technical University of Braunschweig where he studied physical processes at welding electrodes. From 1993 to 1999, he was with the research group „Electrode Processes" at the Institute of Physics, Humboldt-University Berlin and engaged in research on vacuum arcs and high-pressure discharges. From 2000 to 2001, he has been working at the Institute of Low Temperature Plasma Physics in Greifswald. From 2001 to 2016, he was with Eaton Industries GmbH in Bonn where he was involved in research related to circuit breaker development.

Jürgen Sachtleben was born in Roitzsch, Germany, in 1950. He received the degree in physics from Ernst-Moritz-Arndt-University Greifswald in 1973. In 1982, he obtained a second degree in microprocessor technology from Technical University Dresden. From 1978 to 2013, he was the head of the electronics R&D department at the Max-Planck-Institut for Plasma Physics, Subdivision Greifswald.

Martin Balden got his Diploma (Physics) from the Technical University of Aachen (RWTH) in 1992. His PhD-work was on hydrogen absorption on tungsten (110) made at the Forschungszentrum Jülich, Germany. In 1996, he received the Dr. rer. nat. (Physics) at Technical University of Aachen (RWTH). Since 1996, he works as a scientist at the Max-Planck-Institut für Plasmaphysik, Garching, Germany, with the research focused on material characterisation, especially scanning electron microscopy, mainly on carbon and tungsten-based materials and on samples exposed to fusion plasmas.

Volker Rohde was born on 19th of February 1961, in Preetz, Germany. He received his Dr. rer. nat. degree in plasma physics from the Christian Albrechts University, Kiel in 1993. In 1993, he took up a Postdoc position at the Max-Planck-Institut für Plasmaphysik (IPP) in Berlin, Germany, and in 1997, he changed to Garching. He is responsible for vacuum systems and wall conditioning at the tokamak experiment ASDEX Upgrade. His research focus is on plasma wall interaction, neutral gas analysis and erosion processes.

Rudolf Neu was born on 28th of June 1961, in Tübingen, Germany. He received his Dr. rer. nat. degree in nuclear physics from the University of Tübingen in 1992. 2011, he was appointed associate professor at the University of Tübingen and January 2014 he was appointed as professor for plasma material interaction at the Technical University of Munich. In 1992, he took up a Postdoc position at the Max-Planck-Institut für Plasmaphysik (IPP) in Garching, Germany, and in 2006, he was appointed Group Head. During 2012 – 2013, he was head of the ITER physics department of the European Fusion Development Agreement (EFDA) and from 2014, on he returned to IPP as a Group Head and leader of the plasma wall interaction activities. Also, in 2014 he became editor of the journal 'Fusion Engineering and Design'(Elsevier) and was selected for the ISI list of 'Highly Cited Researchers' in the category 'Engineering'.